JACS
JOURNAL OF THE AMERICAN CHEMICAL SOCIETY
Communication
pubs.acs.org/JACS

Dumbbells of Five-Connected Silicon Atoms and Superconductivity in the Binary Silicides MSi_3 (M = Ca, Y, Lu)

Ulrich Schwarz,* Aron Wosylus,† Helge Rosner, Walter Schnelle, Alim Ormeci, Katrin Meier, Alexey Baranov, Michael Nicklas, Susann Leipe, Carola J. Müller, and Yuri Grin

Max-Planck-Institut für Chemische Physik fester Stoffe, 01187 Dresden, Germany

Supporting Information

ABSTRACT: The new metastable binary silicides MSi_3 (M = Ca, Y, Lu) have been synthesized by high-pressure, high-temperature reactions at pressures between 12(2) and 15(2) GPa and temperatures from 900(100) to 1400(150) K. The atomic patterns comprise intricate silicon layers of condensed molecule-like Si_2 dimers. The alkaline-earth element adopts the oxidation state +2, while the rare-earth and transition metals realize +3. All of the compounds exhibit BCS-type superconductivity with weak electron−phonon coupling below critical temperatures of up to 7 K.

The consequent development of in situ high-pressure technology has substantially expanded the map of high-temperature superconductors as much as it has stimulated profound studies of the underlying principles.[1] These phases often expand the spectrum of atomic arrangements in solids by providing access to configurations with unusual and normally enhanced coordination numbers. These local atomic environments can play a decisive role in numerous physical properties. For example, the expanded coordination spheres of compacted phases often provide sufficient dispersion of the bands to induce metallization. In framework compounds, the combination of homopolar interactions with significant charge-carrier concentrations gives rise to the character of a covalent metal, a scenario most favorable for phonon-mediated high-temperature superconductivity.

A method for accessing the beneficial effects of compression at ambient pressure is provided by synthesizing metastable compounds under extreme conditions.[2] In this work, we investigated the potential of silicon-based motifs by combining efforts on high-pressure, high-temperature preparation and on total energy calculations, which yielded new framework compounds MSi_3 housing a large variety of metallic elements (M = Ca, Y, Lu). From the already extensive family of silicon networks, we first developed the novel compound $CaSi_3$ by systematically exploring binary metal−silicon mixtures under high-pressure, high-temperature conditions. The new silicide was synthesized from $CaSi_2$ and Si(*cF*8) (Alpha Aesar, 99.9999%) at pressures between 12(2) and 15(2) GPa and temperatures from 900(100) to 1400(150) K. The crystal structure motif is isotypic to that of the recently described $CaGe_3$[3] and involves two types of Si_2 dumbbell species [Figure 1; also see the Supporting Information (SI)]. Within these diatomic groups, the refined short interatomic distances are

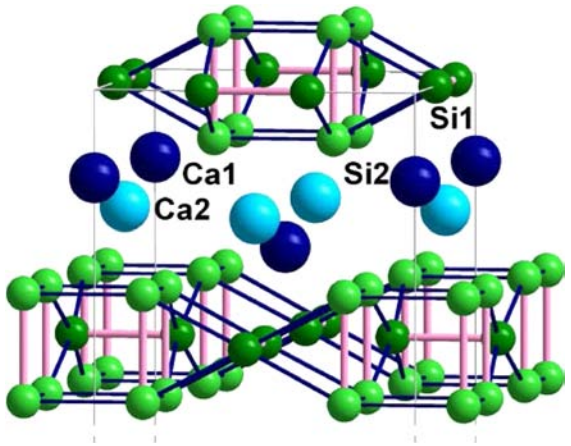

Figure 1. Crystal structure of $CaSi_3$ and the isotypic trisilicides YSi_3 and $LuSi_3$ synthesized at elevated pressures and temperatures. Green spheres indicate silicon atoms, and blue spheres indicate metal atoms. The connectivity of the silicon framework is indicated by colored lines: nearest-neighbor distances d(Si1−Si1) = 239.0(1) pm and d_{SH}(Si2−Si2) = 240.37(8) pm (pink) and longer near-neighbor contacts d(Si1−Si2) = 258.39(9) pm and d_L(Si2−Si2) = 270.37(6) pm (blue). Twelve M−Si distances per metal atom cover the range from 307.88(2) to 331.80(5) pm for $CaSi_3$.

well-compatible with covalent single bonds. Four significantly longer contacts aggregate the isolated dimers into intricate layers that are separated by the calcium atoms. According to the results of ab initio band structure computations,[4] the robust structure pattern of silicon tolerates a broad variety of metallic components. Target-oriented subsequent syntheses yielded isotypic variants such as $LuSi_3$ and YSi_3 (see the SI) under high-temperature, high-pressure conditions similar to those used to manufacture the calcium prototype.[5]

The fivefold connectivity of the silicon atoms impeded the application of the empirical $8 - N$ rule (where N is the number of valence electrons) or the elementary Zintl concept[6] for correlating the electron count with the chemical bonding. Thus, a relevant picture of covalent interactions required elaborate quantum-mechanical calculations. Herein, quantities operating directly in real space, such as the electron localizability indicator (ELI)[7] and the charge density, were combined with k-space tools such as the electronic density of states (DOS).[8] The value of the ELI-D functional[9] is proportional to the electronic

Received: June 7, 2012
Published: July 30, 2012

   dx.doi.org/10.1021/ja3055194 | *J. Am. Chem. Soc.* 2012, 134, 13558−13561

population required for the formation of same-spin electron pairs around certain points in space. The distribution of the ELI is spherically symmetric for noninteracting free atoms. In contrast, local maxima of the ELI, especially in the valence region, are fingerprints of covalent bonding.[10] In $CaSi_3$, the shapes of the ELI domains around the centers of the Si dumbbells (Figure 2b,c) clearly indicate covalent two-center

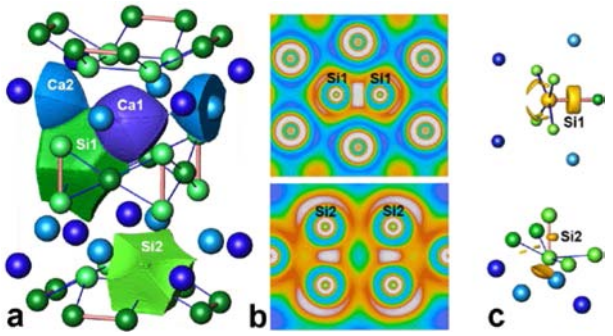

Figure 2. Chemical bonding in $CaSi_3$. (a) Atomic shapes evaluated applying the QTAIM technique.[11] The integration of the electron density within these volumes yields the electron populations of the calcium (18.7 e^- and 18.5 e^-) and silicon (14.4 e^- and 14.5 e^-) atoms. (b) ELI-D distributions within the Si_2 dumbbells and around the Ca atoms, with maxima shown in white revealing covalently bonded silicon dimers. (c) Isosurfaces of high ELI-D values around the Si1 and Si2 atoms, visualizing the positions and shapes of the maxima indicating bonding character for the short (pink) Si−Si contacts. Additional maxima in the region of the long contacts (blue) provide evidence for covalent Si−Si interactions involving Ca−Si contributions.

bonding. Integration of the electron density in the regions assigned to these homopolar interactions yielded 2.1 and 2.2 electrons for the Si1−Si1 and Si2−Si2 contacts, respectively. In agreement with the refined interatomic distances, this is consistent with conventional two-center, two-electron bonds. Interestingly, similar pair formation was observed previously in a high-pressure modification of elemental silicon, Si(*oC*16).[12] In the regions opposite to the bonds within the dumbbells, additional maxima were found (Figure 2b,c). For an isolated Si_2 pair, such a feature would represent lone-pair-like behavior, as was shown earlier for discrete molecules such as N_2[10] and Ge_2.[13] In $CaSi_3$, however, these characteristic domains visualize multicenter interactions involving the calcium atoms. This attribution was supported by the partial DOS contributions (Figure 3), which revealed hybridization of Si 3p and Ca 3d orbitals, mainly in some of the bands crossing the Fermi energy and in the energy range between −2 and −1 eV. Integration of the electron density within the atomic volumes using the quantum theory of atoms in molecules (QTAIM) technique[11] (Figure 2 a) yielded charges of +1.3 and +1.5 for the calcium atoms and −0.4 and −0.5 for silicon, respectively. These values are typical for strongly polar framework compounds (e.g., $Mg^{1.4+}[B^{0.7-}]_2$[14]) and are well in line with the electronegativity differences of the constituent elements.

In agreement with the calculated charge transfer, measurements of the physical properties[15] revealed diamagnetism of MSi_3 (M = Ca; Y; Lu), indicating oxidation states of +2 for calcium and +3 for yttrium and lutetium. At low temperatures, distinctive anomalies in the magnetic susceptibility signaled transitions into the superconducting state. In small magnetic fields, the shielded volume fractions, with uncorrected values of

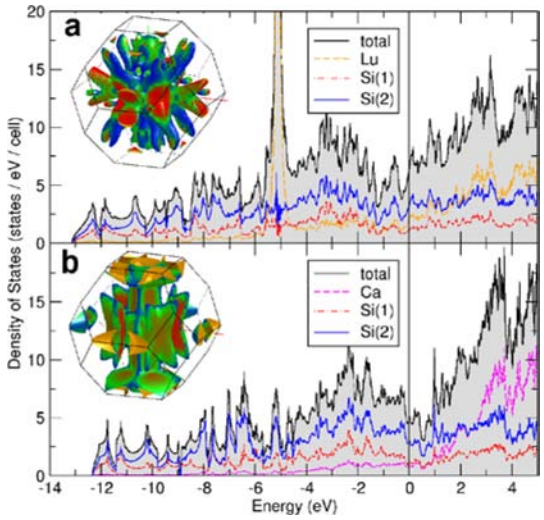

Figure 3. Density of states with partial contributions of the metal and the silicon atoms as well as the Fermi surfaces of (a) $LuSi_3$ and (b) $CaSi_3$. The Fermi velocities (indicated by the coloring from blue to red for increasing values) evidence a reduction of the anisotropy with increasing metal contributions in proceeding from $CaSi_3$ to $LuSi_3$.

1.4 for $CaSi_3$ and YSi_3 and 2.1 for $LuSi_3$, indicated bulk superconductivity with critical temperatures (T_c) ranging from 4.50(5) K for $CaSi_3$ to 7.1(1) K for $LuSi_3$ (see the SI). For comparison, electrical resistance data indicated onset temperatures of 4.5(3) K for $CaSi_3$ and 7.0(3) K for $LuSi_3$, which represents the hitherto only superconducting phase in the Lu−Si system. The bulk character of the superconductivity was confirmed for all of the compounds by specific heat data (Figure 4). The specific heat anomalies associated to the transitions were determined as the differences Δc between the superconducting-state data $c_S(T)$ and the normal-state data $c_{N,fit}(T)$ in the vicinity of T_c. With Sommerfeld coefficients (γ_{exp}) describing the normal-state electronic contribution to the

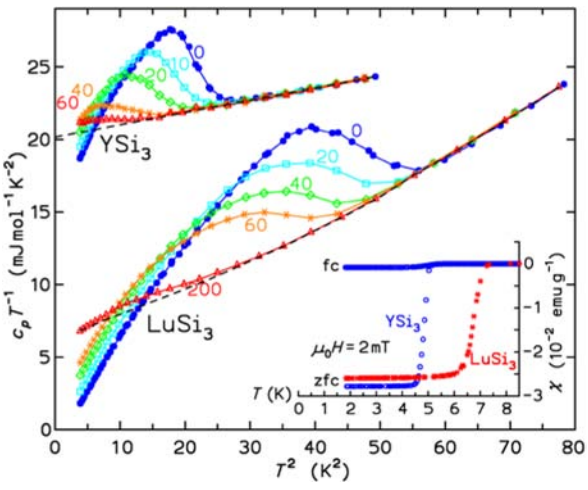

Figure 4. Specific heat capacity (plotted as c_p/T vs T^2) for $LuSi_3$ and YSi_3 (vertically shifted by 15 mJ mol^{-1} K^{-2}) at different magnetic fields (values in mT). Extrapolation revealed that suppression of the superconductivity required upper critical magnetic fields $\mu_0 H_{c2}$ of 234(5) and 80(3) mT for $LuSi_3$ and YSi_3, respectively. The inset shows the magnetic susceptibility, which displays shielding [zero-field cooling (zfc)] and the Meissner effect [field cooling (fc)], indicating superconductivity.

dx.doi.org/10.1021/ja3055194 | J. Am. Chem. Soc. 2012, 134, 13558−13561

specific heat, ratios $\Delta c/\gamma_{exp}T_c$ of 1.41 for YSi_3 and 1.50 for $LuSi_3$ were calculated. The resulting numbers are in accordance with the value of 1.43 predicted by the Bardeen–Cooper–Schrieffer (BCS) theory for weak electron–phonon coupling.

To identify the specific electronic states associated with superconductivity, the total and partial DOS were analyzed in detail (Figure 3; also see the SI). In all of the compounds, the lower part of the valence band (below −6 eV) is dominated by bonding silicon states, and the two species Si1 and Si2 behave rather similarly. For YSi_3 and $LuSi_3$, the contribution of the metal atoms is larger for those parts of the valence band that are closer to the Fermi level, and at E_F it is even larger than the Si contribution per atom. The hybridization of metal d states near E_F with the Si 3p bands indicates important participation in the superconductivity. This statement holds to a lesser extent for the related compound $CaSi_3$. Despite the pronounced similarity of the network-related silicon bands, the participation of metal-connected d states impedes a simple rigid-band approach. For substantial d contributions, the calculated total DOS at E_F (1.7 states per eV and formula unit) in conjunction with the experimental Sommerfeld coefficient γ_{exp} allows to estimate the electron–phonon coupling strength. Within the theory of conventional electron–phonon-coupled superconductivity (a short systematic discussion is given in a recent study[16]), the resulting λ values of 0.6 for YSi_3 and 0.65 for $LuSi_3$ are in line with sizable coupling that facilitates the formation of Cooper pairs even for moderate densities of states at the Fermi level.

The topology of the bands and Fermi surfaces (Figure 3) shows for all of the MSi_3 compounds considerable anisotropy, with the dispersion being significantly stronger within the plane of the layers than perpendicular to them. The ratios of the computed Fermi velocities parallel and orthogonal to the covalent units varied from 2.9 in $CaSi_3$ to 1.4 in $LuSi_3$. With the rather unique situation that the silicon network remains essentially the same despite the chemical diversity of the involved metal atoms, the theoretical findings effectively filter out the relevance of metal d contributions for the direction dependence of the physical properties. This identification is considered an essential component for the effective tailoring of metal–network interactions in structure families of phonon-driven high-T_c materials. Moreover, the theory-guided realization of BCS-type electron–phonon coupling in these emergent metal–network ensembles underlines that combining high-pressure synthesis techniques with predictive theoretical analysis offers significant potential for the materials chemistry of metastable covalent metals.

■ ASSOCIATED CONTENT

Supporting Information

Figures S1–S8 and Tables S1–S4. This material is available free of charge via the Internet at http://pubs.acs.org.

■ AUTHOR INFORMATION

Corresponding Author

schwarz@cpfs.mpg.de

Present Address

[†]BASF AG, 67056 Ludwigshafen, Germany.

Notes

The authors declare no competing financial interest.

■ ACKNOWLEDGMENTS

We thank Susann Leipe for high-pressure syntheses; Yurii Prots, Andreas Czulucki, Irene Margiolaki (ESRF), and Caroline Curfs (ESRF) for synchrotron X-ray diffraction experiments; Stefan Hoffmann and Susann Scharsach for differential thermal analysis measurements; and Dr. Steffen Wirth for competent discussions and critical reading of the manuscript.

■ REFERENCES

(1) (a) Shimizu, K.; Ishikawa, H.; Takao, D.; Yagi, T.; Amaya, K. *Nature* **2002**, *419*, 597–599. (b) Struzhkin, V. V.; Eremets, M. I.; Gan, W.; Mao, H.-K.; Hemley, R. J. *Science* **2002**, *298*, 1213–1215. (c) Kasinathan, D.; Kunes, J.; Lazicki, A.; Rosner, H.; Yoo, C. S.; Scalettar, R. T.; Pickett, W. E. *Phys. Rev. Lett.* **2006**, *96*, No. 047004. (d) Medvedev, S.; McQueen, T. M.; Troyan, I. A.; Palasyuk, T.; Eremets, M. I.; Cava, R. J.; Naghavi, S.; Casper, F.; Ksenofontov, V.; Wortmann, G.; Felser, C. *Nat. Mater.* **2010**, *8*, 630–633. (e) Buzea, C.; Robbie, K. *Supercond. Sci. Technol.* **2005**, *18*, R1–R8. (f) Schilling, J. S. *Physica C* **2005**, *460–462*, 182–185. (g) Shimizu, K.; Kimura, T.; Furomoto, S.; Takeda, K.; Kontani, K.; Onuki, Y.; Amaya, K. *Nature* **2001**, *412*, 316–318. (h) Yabuuchi, T.; Matsuoka, Y.; Shimizu, K. *J. Phys. Soc. Jpn.* **2006**, *75*, No. 083703. (i) Affronte, M.; Sanfilippo, S.; Nunez-Regueiro, M.; Laborde, O.; LeFloch, S.; Bordet, P.; Hanfland, M.; Levi, D.; Palenzona, A.; Olcese, G. L. *Physica B* **2000**, *284–288*, 1117–1118.

(2) (a) Fukuoka, H.; Yamanaka, S. *Phys. Rev. B* **2003**, *67*, No. 094501. (b) Fukuoka, H.; Tomomitsu, Y.; Inumaru, K. *Inorg. Chem.* **2011**, *50*, 6372–6377. (c) Fukuoka, H.; Suekuni, K.; Onimaru, T.; Inumaru, K. *Inorg. Chem.* **2011**, *50*, 3901–3906. (d) Wosylus, A.; Meier, K.; Prots, Yu.; Schnelle, W.; Rosner, H.; Schwarz, U.; Grin, Yu. *Angew. Chem., Int. Ed.* **2010**, *49*, 9002–9006.

(3) Schnelle, W.; Ormeci, A.; Wosylus, A.; Meier, K.; Grin, Yu.; Schwarz, U. *Inorg. Chem.* **2012**, *51*, 5509–5511.

(4) FPLO-9.01-34: Koepernik, K.; Eschrig, H. *Phys. Rev. B* **1999**, *59*, 1743–1757.

(5) Precursors with composition M:Si = 1:2 were prepared by inductive heating of the metals with Si(*cF*8) (Alpha Aesar, 99.9999%) in sealed tantalum ampoules. Next, 1:1 mixtures of the disilicides and Si(*cF*8) were treated at pressures between 12(2) and 15(2) GPa and temperatures from 900(100) to 1400(150) K, yielding the trisilicides MSi_3 (M = Ca, Y). The synthesis of $LuSi_3$ was performed using excess silicon, corresponding to a Lu:Si ratio of 1:5. Pressures were generated within Walker modules encapsulating MgO octahedra. Elevated temperatures were realized by resistive heating of graphite sleeves enclosing h-BN sample crucibles. Sample handling (except for the high-pressure experiments) was performed in argon-filled glove boxes (MBraun, H_2O, O_2 < 0.1 ppm). Crystallographic data: Space group *I*4/*mmm* (No. 139), *Z* = 8. $CaSi_3$: *a* = 726.76(4) pm, *c* = 1135.01(7) pm; Ca1 (0, 0, 0.17384(7)), U_{iso} = 99(2) pm^2; Ca2 (1/2, 0, 1/4), U_{iso} = 113(2) pm^2; Si1 (0.3356(1), 0, 0), U_{iso} = 66(2) pm^2; Si2 (0.31399(6), *x*, 0.10589(5)), U_{iso} = 121(2) pm^2; R_P = 0.029, R_{wp} = 0.036, R_{exp} = 0.009. YSi_3: *a* = 723.10(3) pm, *c* = 1079.2(1) pm; Y1 (0, 0, 0.17050(9)), U_{iso} = 66(3) pm^2; Y2 (1/2, 0, 1/4), U_{iso} = 63(3) pm^2; Si1 (0.3295(3), 0, 0), U_{iso} = 102(5) pm^2; Si2 (0.3141(1), *x*, 0.1117(1)), U_{iso} = 110(4) pm^2; R_P = 0.083, R_{wp} = 0.115, R_{exp} = 0.101. $LuSi_3$: *a* = 718.35(8) pm, *c* = 1047.1(1) pm; Lu1 (0, 0, 0.1683(1)), U_{iso} = 253(2) pm^2; Lu2 (1/2, 0, 1/4), U_{iso} = 254(2) pm^2; Si1 (0.3309(6), 0, 0), U_{iso} = 270(10) pm^2; Si2 (0.3126(2), *x*, 0.1167(2)), U_{iso} = 259(9) pm^2; R_P = 0.054, R_{wp} = 0.076, R_{exp} = 0.037. Details of data collection and refinement and interatomic distances are given in the SI.

(6) (a) Hume-Rothery, W. *Philos. Mag.* **1931**, *11*, 649–678. (b) Zintl, E.; Brauer, G. *Z. Phys. Chem., Abt. B* **1933**, *20*, 245–271. (c) Zintl, E. *Angew. Chem.* **1939**, *52*, 1–6. (d) Klemm, W.; Fricke, H. *Z. Anorg. Allg. Chem.* **1955**, *282*, 162–168. (e) Busmann, E. *Z. Anorg. Allg. Chem.* **1961**, *313*, 90–106. (f) Schäfer, H.; Eisenmann, B.; Müller, W. *Angew. Chem., Int. Ed. Engl.* **1973**, *12*, 694–712. (g) von Schnering, H. G.

Angew. Chem., Int. Ed. Engl. **1981**, *20*, 33−51. (h) Nesper, R. *Prog. Solid State Chem.* **1990**, *20*, 1−45. (i) *Chemistry, Structure, and Bonding of Zintl Phases and Ions*; Kauzlarich, S., Ed.; VCH Publishers: New York, 1996.

(7) (a) Kohout, M. *Int. J. Quantum Chem.* **2004**, *97*, 651−658. (b) Butovskii, M. V.; Döring, Ch.; Bezugly, V.; Wagner, F. R.; Grin, Yu.; Kempe, Rh. *Nat. Chem* **2010**, *2*, 741−744.

(8) Electronic structure calculations and bonding analyses were carried out for $CaSi_3$, YSi_3, and $LuSi_3$ with density functional codes employing the local density approximation in scalar relativistic calculations using the tight-binding linear muffin-tin orbital method within the atomic sphere approximation (TB-LMTO-ASA[17]), full-potential local orbital (FPLO-9.01-34[4]) and APW+lo+LO Elk[18] program packages. For the TB-LMTO calculations, corrections for the overlap of atomic spheres were included.[19] Basis sets containing Ca(4s, 3d), Y(5s, 4d), Lu(6s, 5d, 4f), and Si(3s, 3p) orbitals were selected, with the Ca(4p), Y(5p, 4f), Lu(6p), and Si(3d) functions being down-folded. In the Elk calculations, an APW+lo+LO basis set was employed, and the R × Gkmax parameter was set equal to 8, with the muffin-tin-sphere radii chosen as 1.164 Å for Ca and 0.9525 Å for Si. The ELI was evaluated in the ELI-D representation[9] using ELI modules within the TB−LMTO−ASA[17] and FPLO[20] program packages. The calculations and topological analyses of the ELI-D distribution based on the Elk code were done on a discrete grid[21] with mesh size of ∼0.0265 Å.

(9) (a) Kohout, M.; Wagner, F. R.; Grin, Yu. *Int. J. Quantum Chem.* **2006**, *106*, 1499−1507. (b) Wagner, F. R.; Bezugly, V.; Kohout, M.; Grin, Yu. *Chem.—Eur. J.* **2007**, *13*, 5724−5741.

(10) Wagner, F. R.; Kohout, M.; Grin, Yu. *J. Phys. Chem. A* **2008**, *112*, 9814−9828.

(11) Bader, R. F. W. *Atoms in Molecules: A Quantum Theory*. Clarendon Press: Oxford, U.K., 1990.

(12) (a) Hanfland, M.; Schwarz, U.; Syassen, K.; Takemura, K. *Phys. Rev. Lett.* **1999**, *82*, 1197−1200. (b) Christensen, N. E.; Novikov, D. L.; Methfessel, M. *Solid State Commun.* **1999**, *110*, 615−619. (c) Schwarz, U.; Jepsen, O.; Syassen, K. *Solid State Commun.* **2000**, *113*, 643−648.

(13) Kohout, M.; Wagner, F. R.; Grin, Yu. *Theor. Chem. Acc.* **2002**, *108*, 150−156.

(14) Tsirelson, V.; Stash, A.; Kohout, M.; Rosner, H.; Mori, H.; Sato, S.; Lee, S.; Yamamoto, A.; Tajima, S.; Grin, Yu. *Acta Crystallogr.* **2003**, *B59*, 575−583.

(15) The magnetic susceptibility $\chi(T) = M(T)/H$ was measured in external fields $\mu_0 H$ between 2 mT and 7 T at temperatures of 1.8 K−400 K in a SQUID magnetometer (MPMS XL-7, Quantum Design). The electrical resistivity $\rho(T)$ was determined by a four-probe method. Because of the small size of the samples, the uncertainty in ρ was estimated to be ±20%. For $CaSi_3$, additional measurements (1.8−10 K) at a lower current density ($j \approx 8 \times 10^{-3}$ A mm^{-2}) were performed in magnetic fields. Heat capacity data for $T > 1.9$ K were collected with a relaxation-type method (PPMS, Quantum Design) in fields $\mu_0 H$ below and above the upper critical field of the superconducting phases. Measurements on $CaSi_3$ and important physical properties of MSi_3 (M = Ca, Y, Lu) are compiled in the SI.

(16) Pickett, W. E. *Physica C* **2008**, *468*, 126.

(17) Jepsen, O., Burkhardt, A., Andersen, O. K. *TB-LMTO-ASA*, version 4.7; Max-Planck-Institut für Festkörperforschung: Stuttgart, Germany, 1999.

(18) *Elk 2011*, version 1.2.20; http://elk.sourceforge.net.

(19) Andersen, O. K. *Phys. Rev. B* **1975**, *12*, 3060−3083.

(20) Ormeci, A.; Rosner, H.; Wagner, F. R.; Kohout, M.; Grin, Yu. *J. Phys. Chem. A* **2006**, *110*, 1100−1105.

(21) Kohout, M. *DGrid*, version 4.6; Radebeul, Germany, 2011.